Raman spectroscopy of shocked gypsum from a meteorite impact crater

Journal:	*International Journal of Astrobiology*
Manuscript ID	IJA-AR-16-0702.R3
Manuscript Type:	Research Article
Date Submitted by the Author:	n/a
Complete List of Authors:	Brolly, Connor; University of Aberdeen, Geology & Petroleum Geology Parnell, John; University of Aberdeen, Geology Bowden, Stephen; University of Aberdeen, Geology
Keyword:	Raman spectroscopy, habitability, shocked gypsum, impact crater

Raman spectroscopy of shocked gypsum from a meteorite impact crater

CONNOR BROLLY* [1], JOHN PARNELL [1] & STEPHEN BOWDEN [1]

[1] University of Aberdeen, Department of Geology & Petroleum Geology

*Corresponding author. Tel.: +44 1224 273433; fax: +44 1224272785. E-mail address: c.brolly@abdn.ac.uk

Abstract. Impact craters and associated hydrothermal systems are regarded as sites within which life could originate on Earth, and on Mars. The Haughton impact crater, one of the most well preserved craters on Earth, is abundant in Ca-sulphates. Selenite, a transparent form of gypsum, has been colonised by viable cyanobacteria. Basement rocks which have been shocked are more abundant in endolithic organisms, when compared with un-shocked basement. We infer that selenitic and shocked gypsum are more suitable for microbial colonisation and have enhanced habitability. This is analogous to many Martian craters, such as Gale Crater which has sulphate deposits in a central layered mound, thought to be formed by post-impact hydrothermal springs.

In preparation for the 2020 ExoMars mission, experiments were conducted to determine whether Raman spectroscopy can distinguish between gypsum with different degrees of habitability. Ca-sulphates were analysed using Raman spectroscopy and results show no significant statistical difference between gypsum that has experienced shock by meteorite impact and gypsum which has been dissolved and re-precipitated as an evaporitic crust. Raman spectroscopy is able to distinguish between selenite and unaltered gypsum. This shows that Raman spectroscopy can identify more habitable forms of gypsum, and demonstrates the current capabilities of Raman spectroscopy for the interpretation of gypsum habitability.

Key words: Raman spectroscopy, habitability, shocked gypsum, impact crater

1 Introduction

1.1 Impact generated sulphate deposits and significance for life

Hydrothermal deposits within craters on Mars represent one of the most important targets in the search for life on Mars (Cabrol et al. 1999; Newsom et al. 2001). Hydrothermal systems are realistic sites to sustain life due to the presence of liquid H_2O, heat and dissolved nutrients and alkaline vents within these systems are considered to be locations where life could originate (Farmer & Des Marais 1999; Osinski et al. 2005; Newsom et al. 2001; Lane & Martin 2012). Over 60 impact craters with associated hydrothermal activity have been discovered on Earth, and given the long bombardment history of Mars, impact craters could be a common site to search for life (Chapman & Jones 1977; Naumov 2002). Gale Crater has sulphates present within a layered sedimentary mound in the centre of the crater, named Mount Sharp, thought to be formed by hydrothermal springs, as there is a lack of features associated with lacustrine environments such as terraces, deltas and fans. (Rossi et al. 2008; Thomson et al. 2011; Schwenzer et al. 2012). Semi-hydrated Ca-sulphate, bassanite has been identified in Mawrth Vallis, one of the proposed landing sites for the ExoMars 2020 mission (Wray et al. 2010).

The Eocene Haughton impact crater, located on Devon Island in the Canadian High Arctic Archipelago, provides a useful analogue site to study post impact sulphate deposits (Sherlock et al. 2005). It is exceptionally well preserved, which is why it has been extensively studied, and has examples of sulphate deposits containing microbial life (Osinski & Spray 2001; Parnell et al. 2004). The current structure is composed of a central uplift overlaid with melt breccia which is the most common impactite (Lindgren et al. 2009). There is a gneissic crystalline basement which is shocked and is inhabited by endolithic photosynthetic microorganisms. These organisms are more abundant in the shocked material due to an increased pore space as a result of impact fracturing, and increased translucence due to vaporization of opaque mineral phases (Cockell et al. 2002). The target rock included gypsum bearing carbonate rocks, Ordovician in age (Robertson & Sweeney 1983). Impact remobilised sulphate occurs as selenite, a transparent form of gypsum ($CaSO4\cdot2(H2O)$), which cross-cuts the melt breccia as veins. Viable, extant cyanobacterial colonies are present within the selenite and are black in colour due to the UV protective pigments scytonemin and gloeocapsin (Cockell et al. 2002; Cockell et al. 2003b). Mobilisation still occurs at present in the form of evaporitic crusts on bedrock surfaces and soil (Parnell et al. 2004).

Given that sulphates formed by hydrothermal activity are habitable substrates, and that shocking increases the space for an organism to exploit; shocked sulphates are important targets with which to find evidence of microbial life. If instrumentation could distinguish between shocked and un-shocked phases, and between various sulphate phases, this would be beneficial when identifying the most likely sulphates to contain life signatures.

1.2 Raman for Mars

Raman spectroscopy uses a monochromatic laser light source to irradiate a sample. Majority of the light which interacts with the sample is scattered elastically, with no change in wavelength. However a small proportion of the light is scattered inelastically – either an increase or decrease in wavelength, known as Raman scattering. Raman spectroscopy produces a vibrational 'fingerprint' which is dependent on the vibrational state of molecules in a given compound (Ellery & Wynn-Williams 2003).

The popularity of Raman spectroscopy has dramatically increased in the last 30 years due to its increasing range of applications (Pérez & Martinez-Frias 2006). It is a useful astrobiological tool as it is a non-destructive technique, which is able to be miniaturised. It is sensitive to carbonaceous materials, which is one of the main targets of the ESA ExoMars mission but it is also sensitive to various microbial pigments, such as chlorophylls, carotenoids and scytonemin which increase its appeal (Jehlička et al. 2014; Ellery & Wynn-Williams 2003). It has a wavelength range covering most vibrational modes including carbonates, silicates and sulphates (i.e. most rock-forming minerals), therefore it can also be used for petrographic analysis (Haskin et al. 1997; Wang et al. 1998).

1.3 Raman spectroscopy of gypsum & impact shocked gypsum

The Raman spectrum of gypsum characteristically shows a narrow intense band around 1008 reciprocal centimetres (cm^{-1}) which is the v1 sulphate symmetric stretching mode, herein referred to as v1 sulphate band. The stretching modes of water occur around 3450 cm^{-1} (Krishnamurthy & Soots 1971; Berenblut et al. 1970), shown in figure 1.

Fig. 1 Extended spectra 100-4000 cm^{-1} showing v1 sulphate symmetric stretching mode (1007.89 cm^{-1}) and stretching mode of H_2O (~3450 cm^{-1}).

The astrobiological community is interested in the effect of shocking on sulphates as they occur on Mars. Micro-scale deformation experiments of gypsum by Hogan et al. (2012), show that the v1 sulphate band is least intense at the centre of deformation, where most load was experienced, and most intense at the outer margins of the deformation structure where least load was experienced. This is evidence that shocking reduces the v1 sulphate stretching band intensity. Instantaneous compressional deformation occurs in both meteorite (macro) shock events and micro-indentation experiments.

The effects of shock on gypsum have been discussed by Ramkissoon et al. (2014), using impact shock experiments with a two stage light gas gun and projectile, fired at plaster of Paris (gypsum). Their experiments show that devolatilisation occurs as a result of the impact, based on the disappearance of water molecule bands around 3450 cm^{-1}, and the shift of bands 427 and 487 cm^{-1}, is indicative of anhydrite. Characterising the dehydration of gypsum to anhydrite using Raman spectroscopy has been well studied and shows the sulphate stretching band exhibiting an increase in band position with increasing dehydration (Prasad et al. 2001; Liu et al. 2009).

Bucio et al. (2015) used experimentally impact-shocked gypsum to characterise post-impact phases using Raman spectroscopy and X-Ray diffraction. This study compared Raman spectra obtained from naturally shocked samples with Raman spectra obtained from experimentally impact-shocked gypsum, published by previous authors, to assess if the spectral changes associated with shock are comparable, and ultimately if shocked gypsum can be differentiated from other phases of gypsum. The spectral changes were analysed by comparing v1 sulphate band positions against band widths, referred to as the full width at half maximum (FWHM).

2 Methods

2.1 Samples

Fig 2. Sample photographs. (a) Selenite, Haughton crater (S2), showing black pigmentation of bacterial colonies. (b) Melt breccia, Haughton crater (SH1), showing fragment of shocked gypsum. (c) Evaporitic gypsum crust, Haughton crater (C1).

Gypsum samples were separated into 4 groups:

1. Unaltered gypsum – Samples which have not experienced shock or dissolution and subsequent re-precipitation. The crystal habits range from grainy to massive or fibrous.
2. Selenite - a transparent form of gypsum, which has a distinct platy crystal habit. Selenite at the Haughton structure formed by the dissolution of gypsum in the target rock, and circulated the structure before re-precipitating as selenite.
3. Crusts – sulphate rich waters at the Haughton flows over the surface topography and slowly evaporates, leaving a mineral 'crust' on outcropped rock and soil.
4. Shocked gypsum – samples include a primary shocked gypsum nodule, and shocked gypsum fragments within melt breccia (see figure 2).

The majority of the samples originate from the Haughton impact crater, Devon Island, Canada; see table 1 for more information on sample locations and ages. Minimal sample preparation was employed, simulating capabilities during a remote mission on Mars. If necessary, samples were cut to expose the sulphate, however where possible rough untreated surfaces were analysed. This study would be equally appropriate for the NASA 2020, SHERLOC instrument, which will have spatial mapping capabilities (Beegle et al. 2015).

Table 1. Table of sample locations and ages.

2.2 Raman spectroscopy configuration

Raman spectra were obtained using a Renishaw InVia H36031 confocal Raman microscope operating at a wavelength of 514.5 nm green monochromatic laser light, which is similar to the ExoMars flight instrument wavelength of 532 nm (Rull et al. 2011). The laser power was 0.3 mW, avoiding laser induced heating of samples. A 50 x objective lens was used giving a laser "footprint" of 1-3 µm in diameter, with an extended spectral range of 100 cm^{-1} to 2000 cm^{-1}. 10 seconds exposure time and 1 accumulation were used for each spectrum, giving a good signal-to-noise ratio. To include the stretching modes of water molecules, extended wavelength (100-4000 cm^{-1}) was also measured using the above settings. Spectra were processed using a smooth, baseline subtraction and peak fit functions using WiRE 2.0 software. Peak fitting used a mixture of Gaussian and Lorentzian algorithms.

2.3 X-Ray Diffraction

Diffraction patterns were acquired on powder samples by using an X'Pert diffractometer (PANalytical, NL) equipped with Cu-kα radiation (1.54 Å; 45 kV / 40 mA) in θ-θ reflectance geometry; data were collected from 5 – 80° 2θ with a step size of 0.013° and a time-per-step of 13.77 s. Crystalline phases were identified by comparison to ICDD PDF # [01-074-1433] (Gypsum). Samples were powdered by hand using a pestle & mortar.

2.4 Spectral parameter analysis

10 spectra were obtained from each sample and average FWHM were plotted against sulphate band positions. Statistical variance tests were used to determine if sample groups are statistically different from each another.

2.5 Statistical analysis

Overlapping sample fields were examined using SigmaPlot statistical software package to confirm if the groups were statistically different. The sample groups failed the normality test therefore a non-parametric test was used. As two independent groups were compared, a Man-Whitney U test was used.

3 Results

3.1 Raman spectroscopy

The spectra obtained across the sample set all show a v1 sulphate band position of around 1008 cm^{-1} which is indicative of gypsum (Krishnamurthy & Soots 1971), shown in figure 3. The shocked samples, SH2 & SH3, show a sloping baseline with increased signal-to-noise ratio compared with other samples e.g. selenite. Additionally the shocked samples shows a weaker Raman signal, with lower band intensities. The spectra from evaporitic crusts are similar spectra to that of shocked samples, with low intensity bands and a higher signal-to-noise ratio, a part from the central uplift crust, which has an improved signal-to-noise ratio. The selenite group, have the cleanest spectra with intense v1 sulphate bands and a better signal-to-noise ratio relative to the shocked samples. Unaltered samples show similar spectra to selenite, except from U6 and U5 which have increased signal-to-noise ratios. Average v1 band positions for each are; unaltered (U) – 1009.615, selenite (S) – 1009.261, shocked (SH) – 1008.251, crusts (C) –

1008.262 cm^{-1}. Based on these band positions all samples are classed as gypsum and have not experienced dehydration.

Fig 3. Extended Raman spectra for gypsum (100-2000 cm^{-1}). X axis is Raman shift in reciprocal centimetres (cm^{-1}). Y axis is Raman intensity in arbitrary units (a.u.). 'SH' spectra have experienced shock from meteoric impact. 'C' spectra are gypsum samples which have been dissolved then re-precipitated as evaporitic crusts. 'S' spectra are selenite, a transparent form of gypsum. 'U' spectra are from unaltered gypsum samples unaffected by shock or dissolution and re-precipitation.

3.2 X-ray diffraction

8 gypsum samples were selected from the larger sample set for XRD analysis (figure 4), which cover the 4 Ca-sulphate groups. The cell parameters for each sample show that all 8 samples are in the form of gypsum. It is common for impact shocked sample to experience partial or complete dehydration, however basanite or anhydrite phases are not found in specimen SH3, which is consistent with the Raman measurements obtained.

Fig. 4 X-ray diffraction patterns.

4 Discussion

4.1 Raman spectroscopy - Extended spectra

Selected samples were re-analysed using an extended wavelength range (100-4000 cm^{-1}), to include the stretching modes of water molecules, shown in figure 5. An anhydrite control is included to show a completely dehydrated phase. As expected the anhydrite control shows a v1 sulphate band position of 1015.39 cm^{-}

^{1}, and does not show the stretching modes of water molecules around 3450 cm^{-1}. Sample SH1 has a fragment of gypsum, and the spectrum for shows a v1 band position of 1007.52 cm^{-1} which is indicative of gypsum, although it does not show the presence of water molecules at the expected wavelength. As shocking promotes devolatilisation, the loss of H_2O molecules would be expected, and is well documented by other authors. Additionally, a change in v1 band position from 1008 cm^{-1} to 1015 cm^{-1}, would also be expected. Sample SH2 shows a band position of 1006.24 cm^{-1}, and has the stretching modes of water molecules. This is indicative of gypsum, and suggests that either no dehydration has occurred, or that the specimens have been rehydrated.

Experimental work by Ramkissoon et al. (2014) and Bucio et al. (2015), clearly show that shocking by impact generates, semi-hydrated and completely hydrated Ca-sulphate phases in the form of basanite and anhydrite respectively. This can be seen in the v1 sulphate band positon and the presence, or absence, of the stretching modes of water molecules. This relationship does not appear to be realised in naturally impact shocked Ca-sulphates from Haughton crater.

Fig 5. Extended Raman spectra for gypsum and anhydrite (100-4000 cm^{-1}). Spectra include v1 sulphate stretching mode and H_2O molecule stretching mode around 3500 cm^{-1}.

4.2 v1 band position against band FWHM

The sulphate band position was plotted against the FWHM to determine if these Raman parameters could distinguish between the gypsum specimens. Figure 6(a) shows the 4 types of gypsum used in this study presented as fields. Each point is an average of 10 spectra. Selenite has the largest field which overlaps with unaltered samples. Selenite and unaltered fields plot independently from shocked or crust fields, showing that Raman spectroscopy can distinguish between certain phases of gypsum. The shocked field plots on the edge of the crusts field. Samples with overlapping fields, were analysed for statistical significance. No significant difference was found between the shocked and crust sample band positions ($p=0.966$, Mann-Whitney Sum test) and FWHM ($p=0.251$), indicating that Raman spectroscopy cannot currently distinguish between impact shocked gypsum and gypsum which has been dissolved and re-precipitated as a mineral crust. In contrast, a significant difference is evident between selenite and unaltered sample band positions ($p=0.045$) and FWHM ($p=0.020$). This shows that using the sulphate v1 band position vs WFHM, differences between gypsum phases are evident. Raman can therefore identify gypsum phases with enhanced habitability.

Figure 6(b) distinguishes samples according to their classification in table 1. Figure 6(c) distinguishes samples according to crystal size, which was determined petrographically. However, there does not appear to be any control based on crystal size.

Fig 6. Sulphate band position against sulphate band FWHM, with each point representing an average of 10 spectra. x-axis, is the sulphate (v1) band position in reciprocal centimetres (cm^{-1}). Y-axis, is the sulphate (v1) full width at half maximum (FWHM). (a) Samples are separated into their geological groups. (b) Samples are distinguished by sample classification (table 1). (c) Samples are distinguished based on crystal size. Squares denote a crystal size less than 0.5 cm; diamonds denote a crystal size of between 0.5 and 2 cm; circles denote a crystal size greater than 2 cm.

5 Conclusions

A range of gypsum samples were analysed using Raman spectroscopy, to determine if this technique can differentiate between Ca-sulphates which have enhanced habitability, and those that do not. Results show that Raman spectroscopy cannot currently determine a significant difference between gypsum which has been shocked by meteoric impact (enhancing the habitability), and gypsum which has been dissolved and re-precipitated as an evaporitic crust. Raman spectroscopy is able to differentiate between unaltered gypsum and selenite by plotting v1 sulphate band position against v1 sulphate band FWHM, and as selenite has been found with viable extant microbial colonies at Haughton impact crater, it is regarded as having enhanced habitability.

The presence of H_2O bands in spectra obtained from shocked samples highlights the complexity of Raman spectra observed from naturally shocked samples compared with experimental shock studies. This indicates current capabilities of Raman spectroscopy, for the interpretation of gypsum habitability, prior to its use on the European Space Agency's ExoMars 2020 mission.

Acknowledgements

This work was funded by STFC grant ST/L001233/1. The University of Aberdeen Raman facility was funded by the BBSRC grant BBC5125101. Thanks to Jo Duncan for XRD assistance.

References

Beegle, L. et al., 2015. SHERLOC : Scanning Habitable Environments with Raman & Luminescence for Organics & Chemicals. In *Aerospace Conference*.

Berenblut, B.J., Dawson, P. & Wilkinson, G.R., 1970. The Raman spectrum of gypsum. *Spectrochimica Acta*, 27A, pp.1849–1863.

Bucio, L. et al., 2015. Phase transitions induced by shock compression on a gypsum mineral: X-ray and micro-Raman analysis. *High Pressure Research*, 35(4), pp.355–362.

Cabrol, N.A. et al., 1999. Hydrogeologic evolution of Gale Crater and its relevance to the exobiological exploration of Mars. *Icarus*, 139, pp.235–245.

Chapman, C.R. & Jones, K.L., 1977. Cratering and obliteration history of Mars. *Annual Review of Earth and Planetary Sciences*, 5, pp.515–540.

Cockell, C.S. et al., 2002. Impact-induced microbial endolithic habitats. *Meteoritics & Planetary Science*, 37, pp.1287–1298.

Cockell, C.S. et al., 2003. Measurements of microbial protection from ultraviolet radiation in polar terrestrial microhabitats. *Polar Biology*, 26, pp.62–69.

Ellery, A. & Wynn-Williams, D., 2003. Why Raman spectroscopy on Mars ?— a case of the right tool for the right job. *Astrobiology*, 3(3), pp.565–579.

Farmer, J.D. & Des Marais, D.J., 1999. Exploring for a record of ancient Martian life. *Journal of Geophysical Research*, 104, pp.26,977–26,995.

Haskin, L.A. et al., 1997. Raman spectroscopy for mineral identification and quantificafion for in situ planetary surface analysis : a point count method. *Journal of Geophysical Research*, 102(97), pp.19293–19306.

Hogan, J.D. et al., 2012. Micro-scale deformation of gypsum during micro-indentation loading. *International Journal of Rock Mechanics and Mining Sciences*, 54, pp.140–149.

Jehlička, J., Edwards, H.G.M. & Oren, A., 2014. Raman spectroscopy of microbial pigments. *Applied and environmental microbiology*, 80(11), pp.3286–95.

Krishnamurthy, N. & Soots, V., 1971. Raman spectrum of gypsum. *Canadian Journal of Physics*, pp.71–107.

Lane, N. & Martin, W.F., 2012. The origin of membrane bioenergetics. *Cell*, 151(7), pp.1406–1416.

Lindgren, P. et al., 2009. Preservation of biological markers in clasts within impact melt breccias from the Haughton impact structure, Devon Island. *Astrobiology*, 9(4).

Liu, Y., Wang, A. & Freeman, J.J., 2009. Raman, MIR, and NIR spectroscopic study of calcium sulphates: Gypsum, bassanite, and anhydrite. In *40th Lunar and Planetary Science Conference.* p. 2128.

Naumov, M. V, 2002. Impact-generated hydrothermal systems: Data from Popigai, Kara, and Puchezh-Katunki Impact Structures. In J. Plado & L. J. B. Pesonen, eds. *Impacts in Precambrian Shields*. p. pp 117–171.

Newsom, H.E., Hagerty, J.J. & Thorsos, I.E., 2001. Location and sampling of aqueous and hydrothermal deposits in Martian impact craters. *Astrobiology*, 1(1), pp.71–88.

Osinski, G.R. & Spray, J.G., 2001. Impact-generated carbonate melts: evidence from the Haughton structure, Canada. *Earth and Planetary Science Letters*, 194(1-2), pp.17–29.

Osinski, G.R., Spray, J.G. & Lee, P., 2005. A case study of impact-induced hydrothermal activity: The Haughton impact structure, Devon Island, Canadian High Arctic. *Meteoritics & Planetary Science*, 40(12), pp.1789–1812.

Parnell, J. et al., 2004. Microbial colonization in impact-generated hydrothermal sulphate deposits, Haughton impact structure, and implications for sulphates on Mars. *International Journal of Astrobiology*, 3(3), pp.247–256.

Pérez, F.R. & Martinez-Frias, J., 2006. Raman spectroscopy goes to Mars. *Spectroscopy*

Europe, 18(1), pp.18–21.

Prasad, P.S.R., Pradhan, A. & Gowd, T.N., 2001. In situ micro-Raman investigation of dehydration mechanism in natural gypsum. *Current Science*, 80(9), pp.1203–1207.

Ramkissoon, N.K. et al., 2014. Examining impact induced mineral devolatilisation using Raman spectroscopy. In *45th Lunar and Planetary Science Conference*. p. Abstract 1891.

Robertson, P.B. & Sweeney, J.F., 1983. Haughton impact structure: structural and morphological aspects. *Canadian Journal of Earth Sciences*, 20(7), pp.1134–1151.

Rossi, A.P. et al., 2008. Large-scale spring deposits on Mars? *Journal of Geophysical Research E: Planets*, 113(8), pp.1–17.

Rull, F. et al., 2011. The Raman Laser Spectrometer (RLS) on the ExoMars 2018 Rover Mission. In *42nd Lunar and Planetary Science Conference*.

Schwenzer, S.P. et al., 2012. Gale Crater: Formation and post-impact hydrous environments. *Planetary and Space Science*, 70(1), pp.84–95.

Sherlock, S.C. et al., 2005. Re-evaluating the age of the Haughton impact event. *Meteoritics & Planetary Science*, 40(12), pp.1777–1787.

Thomson, B.J. et al., 2011. Constraints on the origin and evolution of the layered mound in Gale Crater, Mars using Mars Reconnaissance Orbiter data. *Icarus*, 214(2), pp.413–432.

Wang, A., Haskin, L.A. & Cortez, E., 1998. Prototype Raman spectroscopic sensor for in situ mineral characterization on planetary surfaces. *Applied Spectroscopy*, 52(4), pp.477–487.

Wray, J.J. et al., 2010. Identification of the Ca-sulfate bassanite in Mawrth Vallis, Mars. *Icarus*, 209(2), pp.416–421.

Sample	Description/Location	Age	Group
U1	Vale of Eden, Cumbria, UK	Permian	1
U2	Kingscourt fibrous, Co. Cavan, Ireland	Triassic	1
U3	Scapa, Orkney	Devonian	1
U4	Kingscourt with hematite, Co. Cavan, Ireland	Triassic	1
U5	Gotham Triassic, England	Triassic	1
U6	Ebro Basin, Spain	Oligocene-Miocene	1
S1	Selenite, California	Paleogene	2

S2	Selenite, Haughton, Devon Island	Eocene-Oligocene	2
S3	GSC dome (NE side), Selenite Haughton, Devon Island	Eocene-Oligocene	2
S4	Selenite, Kent	Eocene	2
C1	Central uplift crust, Haughton, Devon Island	Eocene-Holocene	3
C2	GSC dome (NE side) crust, Haughton, Devon Island	Eocene-Holocene	3
C3	Gypcrete Chile	Paleogene - Holocene	3
C4	Rhino Creek, Crust on lake sediments, Haughton, Devon Island	Eocene-Holocene	3
SH1	West Rhino creek melt breccia, Haughton, Devon Island	Eocene	4
SH2	Gemini Hills Shocked A Haughton, Devon Island	Eocene	4
SH3	Gemini Hills Shocked B Haughton, Devon Island	Eocene	4

Table 1 Table of sample locations and ages.

Raman spectroscopy of shocked gypsum from a meteorite impact crater

CONNOR BROLLY* [1], JOHN PARNELL [1] & STEPHEN BOWDEN [1]

[1] University of Aberdeen, Department of Geology & Petroleum Geology

*Corresponding author. Tel.: +44 1224 273433; fax: +44 1224272785. E-mail address: c.brolly@abdn.ac.uk

Abstract. Impact craters and associated hydrothermal systems are regarded as sites within which life could originate on Earth, and on Mars. The Haughton impact crater, one of the most well preserved craters on Earth, is abundant in Ca-sulphates. Selenite, a transparent form of gypsum, has been colonised by viable cyanobacteria. Basement rocks which have been shocked are more abundant in endolithic organisms, when compared with un-shocked basement.~~,~~ We infer that ~~therefore~~ selenitic and shocked gypsum are more suitable for microbial colonisation and have enhanced habitability. This is analogous to many Martian craters, such as Gale Crater which has sulphate deposits in a central layered mound, thought to be formed by post-impact hydrothermal springs.

In preparation for the 2020 ExoMars mission, experiments were conducted to determine whether Raman spectroscopy can distinguish between gypsum with different degrees of habitability. Ca-sulphates were analysed using Raman spectroscopy and results show no significant statistical difference between gypsum that has experienced shock by meteorite impact and gypsum which has been dissolved and re-precipitated as an evaporitic crust. Raman spectroscopy is able to distinguish between selenite and unaltered gypsum. This shows that Raman spectroscopy can identify more habitable forms of gypsum, and demonstrates the current capabilities of Raman spectroscopy for the interpretation of gypsum habitability.

Key words: Raman spectroscopy, habitability, shocked gypsum, impact crater

1 Introduction

1.1 Impact generated sulphate deposits and significance for life

Hydrothermal deposits within craters on Mars represent one of the most important targets in the search for life on Mars (Cabrol et al. 1999; Newsom et al. 2001). Hydrothermal systems are realistic sites for life to ariseto sustain life due to the presence of liquid H_2O, heat and dissolved nutrients and alkaline vents within these systems therefore are considered to be locations where primitive life could evolve originate (Farmer & Des Marais 1999; Osinski et al. 2005; Newsom et al. 2001; Lane & Martin 2012). Over 60 impact craters with associated hydrothermal activity have been discovered on Earth, with associated hydrothermal activity and given the long bombardment history of Mars, impact craters could be a common site to search for life (Chapman & Jones 1977; Naumov 2002). Gale Crater has sulphates present within a layered sedimentary mound in the centre of the crater, named Mount Sharp, thought to be formed by hydrothermal springs, as there is a lack of features associated with lacustrine environments such as terraces, deltas and fans. (Rossi et al. 2008; Thomson et al. 2011; Schwenzer et al. 2012). Semi-hydrated Ca-sulphate, bassanite has been identified in Mawrth Vallis, one of the proposed landing sites for the ExoMars 2020 mission (Wray et al. 2010).

The Eocene Haughton impact crater, located on Devon Island in the Canadian High Arctic Archipelago, provides a useful analogue site to study post impact sulphate deposits (Sherlock et al. 2005). It is exceptionally well preserved, which is why it has been extensively studied, and has examples of sulphate deposits containing microbial life (Osinski & Spray 2001; Parnell et al. 2004). The current structure is composed of a central uplift overlaid with melt breccia which is the most common impactite (Lindgren et al. 2009). There is a gneissic crystalline basement which is shocked and is inhabited by endolithic photosynthetic microorganisms. These organisms are more abundant in the shocked material due to an increased pore space as a result of impact fracturing, and increased translucence due to vaporization of opaque mineral phases (Cockell et al. 2002). The target rock included gypsum bearing carbonate rocks, Ordovician in age (Robertson & Sweeney 1983). Impact remobilised sulphate occurs as selenite, a transparent form of gypsum (CaSO4·2(H2O)), which cross-cuts the melt breccia as veins. Viable, extant cyanobacterial colonies are present within the selenite and are black in colour due to the UV protective pigments scytonemin and gloeocapsin (Cockell et al. 2002; Cockell et al. 2003b). Mobilisation still occurs at present in the form of ~~evapouritic~~evaporitic crusts on bedrock surfaces and soil (Parnell et al. 2004).

Given that sulphates formed by hydrothermal activity are ~~regarded as realistic sites for life to evolve~~habitable substrates, and that shocking increases the space for an organism to exploit; ~~this suggests that~~ shocked sulphates are important targets with which to find evidence of microbial life. If instrumentation could distinguish between shocked and un-shocked phases, and between various sulphate phases, this would be beneficial when identifying the most likely sulphates to contain life signatures.

1.2 Raman for Mars

Raman spectroscopy uses a monochromatic laser light source to irradiate a sample. Majority of the light which interacts with the sample is scattered elastically, with no change in wavelength. However a small proportion of the light is scattered inelastically – either an increase or decrease in wavelength, known as Raman scattering. Raman spectroscopy produces a vibrational 'fingerprint' which is dependent on the vibrational state of molecules in a given compound (Ellery & Wynn-Williams 2003).

The popularity of Raman spectroscopy has dramatically increased in the last 30 years due to its increasing range of applications (Pérez & Martinez-Frias 2006). It is a useful astrobiological tool as it is a non-destructive technique, which is able to be miniaturised. It is sensitive to carbonaceous materials, which is one of the main targets of the ESA ExoMars mission but it is also sensitive to various microbial pigments, such as chlorophylls, carotenoids and scytonemin which increase its appeal (Jehlička et al. 2014; Ellery & Wynn-Williams 2003). It has a wavelength range covering most vibrational modes including carbonates, silicates and sulphates (i.e. most rock-forming minerals), therefore it can also be used for petrographic analysis (Haskin et al. 1997; Wang et al. 1998).

1.3 Raman spectroscopy of gypsum & impact shocked gypsum

The Raman spectrum of gypsum characteristically shows a narrow intense band around 1008 reciprocal centimetres (cm^{-1}) which is the v1 sulphate symmetric stretching mode, herein referred to as v1 sulphate band. The stretching modes of water occur around 3450 cm^{-1} (Krishnamurthy & Soots 1971; Berenblut et al. 1970), shown in figure 1.

Fig. 1 Extended spectra 100-4000 cm^{-1} showing v1 sulphate symmetric stretching mode (1007.89 cm^{-1}) and stretching mode of H_2O (~3450 cm^{-1}).

The astrobiological community is interested in the effect of shocking on sulphates as they occur on Mars. Micro-scale deformation experiments of gypsum by

Hogan et al. (2012), show that the v1 sulphate band is least intense at the centre of deformation, where most load was experienced, and most intense at the outer margins of the deformation structure where least load was experienced. This is evidence that shocking reduces the v1 sulphate stretching band intensity. ~~This is analogous because i~~Instantaneous compressional deformation occurs in both meteorite (macro) shock events and micro-indentation experiments.

The effects of shock on gypsum have been discussed by Ramkissoon et al. (2014), using impact shock experiments with a two ~~2~~ stage light gas gun and projectile, fired at plaster of Paris (gypsum). Their experiments show that devolatilisation occurs as a result of the impact, based on the disappearance of water molecule bands around 3450 cm^{-1}, and the shift of bands 427 and 487 cm^{-1}, is indicative of anhydrite. Characterising the dehydration of gypsum to anhydrite using Raman spectroscopy has been well studied and shows the sulphate stretching band exhibiting an increase in band position with increasing dehydration (Prasad et al. 2001; Liu et al. 2009).

Bucio et al. (2015) used experimentally impact-shocked gypsum to~~and~~ characterise ~~s the~~ post-impact phases using Raman spectroscopy and X-Ray diffraction. This study ~~will compare~~compared Raman spectra obtained from naturally shocked samples with Raman spectra obtained from experimentally impact-shocked gypsum, published by previous authors, to assess if the spectral changes associated with shock are comparable, and ultimately if shocked gypsum can be differentiated from other phases of gypsum. The spectral changes ~~will be~~were analysed by comparing v1 sulphate band positions against band widths, referred to as the full width at half maximum (FWHM).

2 Methods

2.1 Samples

Fig 2. Sample photographs. (a) Selenite, Haughton crater (S2), showing black pigmentation of bacterial colonies. (b) Melt breccia, Haughton crater (SH1), showing fragment of shocked gypsum. (c) Evaporitic gypsum crust, Haughton crater (C1).

Gypsum samples were separated into 4 groups:

1. Unaltered gypsum – Samples which have not experienced shock or dissolution and subsequent re-precipitation. The crystal habits range from grainy to massive or fibrous.
2. Selenite - a transparent form of gypsum, which has a distinct platy crystal habit. Selenite at the Haughton structure formed by the dissolution of gypsum in the target rock, and circulated the structure before re-precipitating as selenite.
3. Crusts – sulphate rich waters at the Haughton flows over the surface topography and slowly evaporates, leaving a mineral ‘crust’ on outcropped rock and soil.
4. Shocked gypsum – samples include a primary shocked gypsum nodule, and shocked gypsum fragments within melt breccia~~-~~ (see figure 2).

The majority of the samples originate from the Haughton impact crater, Devon Island, Canada;~~, as it is one of the most well preserved impact craters on Earth,~~ see table 1 for more information on sample locations and ages. Minimal sample preparation was employed, simulating capabilities during a remote mission on

Mars. If necessary, samples were cut to expose the sulphate, however where possible rough untreated surfaces were analysed. This study would be equally appropriate for the NASA 2020, SHERLOC instrument, which will have spatial mapping capabilities (Beegle et al. 2015).

Table 1. Table of sample locations and ages.

2.2 Raman spectroscopy configuration

Raman spectra were obtained using a Renishaw InVia H36031 confocal Raman microscope operating at a wavelength of 514.5 nm green monochromatic laser light, which is similar to the ExoMars flight instrument wavelength of 532 nm (Rull et al. 2011). The laser power was 0.3 mW, avoiding laser induced heating of samples. A 50 x objective lens was used giving a laser "footprint" of 1-3 µm in diameter, with an extended spectral range of 100 cm^{-1} to 2000 cm^{-1}. 10 seconds exposure time and 1 accumulation were used for each spectrum, giving a good signal-to-noise ratio. To include the stretching modes of water molecules, extended wavelength (100-4000 cm^{-1}) was also measured using the above settings. Spectra were processed using a smooth, baseline subtraction and peak fit functions using WiRE 2.0 software. Peak fitting used a mixture of Gaussian and Lorentzian algorithms.

2.3 X-Ray Diffraction

Diffraction patterns were acquired on powder samples by using an X'Pert diffractometer (PANalytical, NL) equipped with Cu-kα radiation (1.54 Å; 45 kV / 40 mA) in θ-θ reflectance geometry; data were collected from 5 – 80° 2θ with a step size of 0.013° and a time-per-step of 13.77 s. Crystalline phases were identified by comparison to ICDD PDF # [01-074-1433] (Gypsum). Samples were powdered by hand using a pestle & mortar.

2.4 Spectral parameter analysis

Formatted: Space Before: 6 pt, After: 6 pt

10 spectra were obtained from each sample and average FWHM were plotted against sulphate band positions. ~~The band position is a parameter which is commonly used to asses dehydration, whereas the FWHM is not commonly assessed. This method was used to determine dehydration but also, even small-scale differences in spectral parameters would be highlighted, indicating if sample groups were different.~~ Statistical variance tests ~~will be~~were used to determine if sample groups are statistically different from each another.

2.5 Statistical analysis

Overlapping sample fields were examined using SigmaPlot statistical software package to confirm if the groups were statistically different. The sample groups failed the normality test therefore a non-parametric test was used. As two independent groups were compared, a Man-Whitney U test was used.

3 Results

3.1 Raman spectroscopy

The spectra obtained across the sample set all show a v1 sulphate band position of around 1008 cm^{-1} which is indicative of gypsum (Krishnamurthy & Soots 1971), shown in figure 3. The shocked samples, SH2 & SH3, show a sloping baseline with increased signal-to-noise ratio compared with other samples e.g. selenite.

Additionally the shocked samples shows a weaker Raman signal, with lower band intensities. The spectra from evaporitic crusts ~~show~~ are similar spectra to that of shocked samples, with low intensity bands and a higher signal-to-noise ratio, a part from the central uplift crust, which has an improved signal-to-noise ratio. The selenite group, have the cleanest spectra with intense v1 sulphate bands and a better signal-to-noise ratio relative to the shocked samples. Unaltered samples show similar spectra to selenite, except from U6 and U5 which have increased signal-to-noise ratios. Average v1 band positions for each are; unaltered (U) – 1009.615, selenite (S) – 1009.261, shocked (SH) – 1008.251, crusts (C) – 1008.262 cm^{-1}. Based on these band positions all samples are classed as gypsum and have not experienced dehydration.

Fig 3. Extended Raman spectra for gypsum (100-2000 cm^{-1}). X axis is Raman shift in reciprocal centimetres (cm^{-1}). Y axis is Raman intensity in arbitrary units (a.u.). 'SH' spectra have experienced shock from meteoric impact. 'C' spectra are gypsum samples which have been dissolved then re-precipitated as evaporitic crusts. 'S' spectra are selenite, a transparent form of gypsum. 'U' spectra are from unaltered gypsum samples unaffected by shock or dissolution and re-precipitation.

3.2 X-ray diffraction

8 gypsum samples were selected from the larger sample set for XRD analysis (figure 4), which cover the 4 Ca-sulphate groups. The cell parameters for each sample show that all 8 samples are in the form of gypsum. It is common for impact shocked sample to experience partial or complete dehydration, however

basanite or anhydrite phases are not found in specimen SH3, which is consistent with the Raman measurements obtained.

Fig. 4 X-ray diffraction patterns.

4 Discussion

4.1 Raman spectroscopy - Extended spectra

Selected samples were re-analysed using an extended wavelength range (100-4000 cm^{-1}), to include the stretching modes of water molecules, shown in figure 5. An anhydrite control is included to show a completely dehydrated phase. As expected the anhydrite control shows a v1 sulphate band position of 1015.39 cm^{-1}, and does not show the stretching modes of water molecules around 3450 cm^{-1}. Sample SH1 has a fragment of gypsum, and the spectrum for shows a v1 band position of 1007.52 cm^{-1} which is indicative of gypsum, although it does not show the presence of water molecules at the expected wavelength. As shocking promotes devolatilisation, the loss of H_2O molecules would be expected, and is well documented by other authors. Additionally, a change in v1 band position from 1008 cm^{-1} to 1015 cm^{-1}, would also be expected. Sample SH2 shows a band position of 1006.24 cm^{-1}, and has the stretching modes of water molecules. This is indicative of gypsum, and suggests that either no dehydration has occurred, or that the specimens have been rehydrated.

Experimental work by Ramkissoon et al. (2014) and Bucio et al. (2015), clearly show that shocking by impact generates, semi-hydrated and completely hydrated Ca-sulphate phases in the form of basanite and anhydrite respectively. This can be seen in the v1 sulphate band positon and the presence, or absence, of the stretching modes of water molecules. This relationship does not appear to be realised in naturally impact shocked Ca-sulphates from Haughton crater.

Fig 5. Extended Raman spectra for gypsum and anhydrite (100-4000 cm^{-1}). Spectra include v1 sulphate stretching mode and H_2O molecule stretching mode around 3500 cm^{-1}.

4.2 v1 band position against band FWHM

The sulphate band position was plotted against the FWHM to determine if these Raman parameters could distinguish between the gypsum specimens. Figure 6(a) shows the 4 types of gypsum used in this study presented as fields. Each point is an average of 10 spectra. Selenite has the largest field which overlaps with unaltered samples. Selenite and unaltered fields plot independently from shocked or crust fields, showing that Raman spectroscopy can distinguish between certain phases of gypsum. The shocked field plots on the edge of the crusts field. Samples with overlapping fields, were analysed for statistical significance. No significant difference was found between the shocked and crust sample band positions ($p=0.966$, Mann-Whitney Sum test) and FWHM ($p=0.251$), indicating that Raman spectroscopy cannot currently distinguish between impact shocked gypsum and gypsum which has been dissolved and re-precipitated as a mineral crust. In contrast, a significant difference is evident between selenite and unaltered sample band positions ($p=0.045$) and FWHM ($p=0.020$). This shows that using the sulphate v1 band position vs WFHM, differences between gypsum phases are evident. Raman can therefore identify gypsum phases with enhanced habitability.

Figure 6(b) distinguishes samples according to their classification in table 1. Figure 6(c) distinguishes samples according to crystal size, which was determined petrographically. However, there does not appear to be any control based on crystal size.

Fig 6. Sulphate band position against sulphate band FWHM, with each point representing an average of 10 spectra. x-axis, is the sulphate (v1) band position in reciprocal centimetres (cm^{-1}). Y-axis, is the sulphate (v1) full width at half maximum (FWHM). (a) Samples are separated into their geological groups. (b) Samples are distinguished by sample classification (table 1). (c) Samples are distinguished based on crystal size. Squares denote a crystal size less than 0.5 cm; diamonds denote a crystal size of between 0.5 and 2 cm; circles denote a crystal size greater than 2 cm.

5 Conclusions

A range of gypsum samples were analysed using Raman spectroscopy, to determine if this technique can differentiate between Ca-sulphates which have enhanced habitability, and those that do not. Results show that Raman spectroscopy cannot currently determine a significant difference between gypsum which has been shocked by meteoric impact (enhancing the habitability), and gypsum which has been dissolved and re-precipitated as an evaporitic crust. Raman spectroscopy is able to differentiate between unaltered gypsum and selenite by plotting v1 sulphate band position against v1 sulphate band FWHM, and as selenite has been found with viable extant microbial colonies at Haughton impact crater, it is regarded as having enhanced habitability.

The presence of H_2O bands in spectra obtained from shocked samples highlights the complexity of Raman spectra observed from naturally shocked samples compared with experimental shock studies. This indicates current capabilities of Raman spectroscopy, for the interpretation of gypsum habitability, prior to its use on the European Space Agency's ExoMars 2020 mission.

Acknowledgements

This work was funded by STFC grant ST/L001233/1. The University of Aberdeen Raman facility was funded by the BBSRC grant BBC5125101. Thanks to Jo Duncan for XRD assistance.

References

Beegle, L. et al., 2015. SHERLOC : Scanning Habitable Environments with Raman & Luminescence for Organics & Chemicals. In *Aerospace Conference*.

Berenblut, B.J., Dawson, P. & Wilkinson, G.R., 1970. The Raman spectrum of gypsum. *Spectrochimica Acta*, 27A, pp.1849–1863.

Bucio, L. et al., 2015. Phase transitions induced by shock compression on a gypsum mineral: X-ray and micro-Raman analysis. *High Pressure Research*, 35(4), pp.355–362. ~~Available at: http://www.tandfonline.com/doi/full/10.1080/08957959.2015.1085034.~~

Cabrol, N.A. et al., 1999. Hydrogeologic evolution of Gale Crater and its relevance to the exobiological exploration of Mars. *Icarus*, 139, pp.235–245. ~~Available at: http://dx.doi.org/10.1006/icar.1999.6099.~~

Chapman, C.R. & Jones, K.L., 1977. Cratering and obliteration history of Mars. *Annual Review of Earth and Planetary Sciences*, 5, pp.515–540.

Cockell, C.S. et al., 2002. Impact-induced microbial endolithic habitats. *Meteoritics & Planetary Science*, 37, pp.1287–1298.

Cockell, C.S. et al., 2003. Measurements of microbial protection from ultraviolet radiation in polar terrestrial microhabitats. *Polar Biology*, 26, pp.62–69.

Ellery, A. & Wynn-Williams, D., 2003. Why Raman spectroscopy on Mars ?— a case of the right tool for the right job. *Astrobiology*, 3(3), pp.565–579.

Farmer, J.D. & Des Marais, D.J., 1999. Exploring for a record of ancient Martian life. *Journal of Geophysical Research*, 104, pp.26,977–26,995.

Haskin, L.A. et al., 1997. Raman spectroscopy for mineral identification and quantificafion for in situ planetary surface analysis : a point count method. *Journal of Geophysical Research*, 102(97), pp.19293–19306.

Hogan, J.D. et al., 2012. Micro-scale deformation of gypsum during micro-indentation loading. *International Journal of Rock Mechanics and Mining Sciences*, 54, pp.140–149. ~~Available at: http://linkinghub.elsevier.com/retrieve/pii/S1365160912001086 [Accessed March 7, 2014].~~

Jehlička, J., Edwards, H.G.M. & Oren, A., 2014. Raman spectroscopy of microbial pigments. *Applied and environmental microbiology*, 80(11), pp.3286–95. ~~Available at: http://www.pubmedcentral.nih.gov/articlerender.fcgi?artid=4018853&tool=pmcentrez&rendertype=abstract.~~

Krishnamurthy, N. & Soots, V., 1971. Raman spectrum of gypsum. *Canadian Journal of Physics*, pp.71–107.

Lane, N. & Martin, W.F., 2012. The origin of membrane bioenergetics. *Cell*, 151(7), pp.1406–1416. ~~Available at: http://dx.doi.org/10.1016/j.cell.2012.11.050.~~

Lindgren, P. et al., 2009. Preservation of biological markers in clasts within impact melt breccias from the Haughton impact structure, Devon Island. *Astrobiology*, 9(4).

Liu, Y., Wang, A. & Freeman, J.J., 2009. Raman, MIR, and NIR spectroscopic study of calcium sulphates: Gypsum, bassanite, and anhydrite. In *40th Lunar and Planetary Science Conference.* p. 2128.

Naumov, M. V, 2002. Impact-generated hydrothermal systems: Data from Popigai, Kara, and Puchezh-Katunki Impact Structures. In J. Plado & L. J. B. Pesonen, eds. *Impacts in Precambrian Shields*. p. pp 117–171.

Newsom, H.E., Hagerty, J.J. & Thorsos, I.E., 2001. Location and sampling of aqueous and hydrothermal deposits in Martian impact craters. *Astrobiology*, 1(1), pp.71–88. ~~Available at: http://adsabs.harvard.edu/cgi-bin/nph-bib_query?bibcode=2001AsBio...1...71N&db_key=AST.~~

Osinski, G.R. & Spray, J.G., 2001. Impact-generated carbonate melts: evidence from the Haughton structure, Canada. *Earth and Planetary Science Letters*, 194(1-2), pp.17–29. ~~Available at: http://linkinghub.elsevier.com/retrieve/pii/S0012821X01005581.~~

Osinski, G.R., Spray, J.G. & Lee, P., 2005. A case study of impact-induced hydrothermal activity: The Haughton impact structure, Devon Island, Canadian High Arctic. *Meteoritics & Planetary Science*, 40(12), pp.1789–1812. ~~Available at: https://www.lib.uwo.ca/cgi-bin/ezpauthn.cgi/docview/50278222?accountid=15115\nhttp://sfx.scholarsportal.info/western?url_ver=Z39.88-2004&rft_val_fmt=info:ofi/fmt:kev:mtx:journal&genre=article&sid=ProQ:ProQ:georefmodule&atitle=Impactites+of+the+Haughton+im.~~

Parnell, J. et al., 2004. Microbial colonization in impact-generated hydrothermal sulphate deposits, Haughton impact structure, and implications for sulphates on Mars. *International Journal of Astrobiology*, 3(3), pp.247–256. Available at: http://www.journals.cambridge.org/abstract_S1473550404001995 [Accessed July 25, 2014].

Pérez, F.R. & Martinez-Frias, J., 2006. Raman spectroscopy goes to Mars. *Spectroscopy Europe*, 18(1), pp.18–21.

Prasad, P.S.R., Pradhan, A. & Gowd, T.N., 2001. In situ micro-Raman investigation of dehydration mechanism in natural gypsum. *Current Science*, 80(9), pp.1203–1207.

Ramkissoon, N.K. et al., 2014. Examining impact induced mineral devolatilisation using Raman spectroscopy. In *45th Lunar and Planetary Science Conference*. p. Abstract 1891.

Robertson, P.B. & Sweeney, J.F., 1983. Haughton impact structure: structural and morphological aspects. *Canadian Journal of Earth Sciences*, 20(7), pp.1134–1151.

Rossi, A.P. et al., 2008. Large-scale spring deposits on Mars? *Journal of Geophysical Research E: Planets*, 113(8), pp.1–17.

Rull, F. et al., 2011. The Raman Laser Spectrometer (RLS) on the ExoMars 2018 Rover Mission. In *42nd Lunar and Planetary Science Conference*.

Schwenzer, S.P. et al., 2012. Gale Crater: Formation and post-impact hydrous environments. *Planetary and Space Science*, 70(1), pp.84–95. Available at: http://dx.doi.org/10.1016/j.pss.2012.05.014.

Sherlock, S.C. et al., 2005. Re-evaluating the age of the Haughton impact event. *Meteoritics & Planetary Science*, 40(12), pp.1777–1787. Available at: http://www.ingentaconnect.com/content/arizona/maps/2005/00000040/00000012/art00003.

Thomson, B.J. et al., 2011. Constraints on the origin and evolution of the layered mound in Gale Crater, Mars using Mars Reconnaissance Orbiter data. *Icarus*, 214(2), pp.413–432. ~~Available at: http://dx.doi.org/10.1016/j.icarus.2011.05.002.~~

Wang, A., Haskin, L.A. & Cortez, E., 1998. Prototype Raman spectroscopic sensor for in situ mineral characterization on planetary surfaces. *Applied Spectroscopy*, 52(4), pp.477–487.

Wray, J.J. et al., 2010. Identification of the Ca-sulfate bassanite in Mawrth Vallis, Mars. *Icarus*, 209(2), pp.416–421. ~~Available at: http://dx.doi.org/10.1016/j.icarus.2010.06.001.~~

Sample	Description/Location	Age	Group
U1	Vale of Eden, Cumbria, UK	Permian	1
U2	Kingscourt fibrous, Co. Cavan, Ireland	Triassic	1
U3	Scapa, Orkney	Devonian	1
U4	Kingscourt with hematite, Co. Cavan, Ireland	Triassic	1
U5	Gotham Triassic, England	Triassic	1
U6	Ebro Basin, Spain	Oligocene-Miocene	1
S1	Selenite, California	Paleogene	2
S2	Selenite, Haughton, Devon Island	Eocene-Oligocene	2
S3	GSC dome (NE side), Selenite Haughton, Devon Island	Eocene-Oligocene	2
S4	Selenite, Kent	Eocene	2
C1	Central uplift crust, Haughton, Devon Island	Eocene-Holocene	3
C2	GSC dome (NE side) crust, Haughton, Devon Island	Eocene-Holocene	3
C3	Gypcrete Chile	Paleogene - Holocene	3
C4	Rhino Creek, Crust on lake sediments, Haughton, Devon Island	Eocene-Holocene	3
SH1	West Rhino creek melt breccia, Haughton, Devon Island	Eocene	4
SH2	Gemini Hills Shocked A Haughton, Devon Island	Eocene	4
SH3	Gemini Hills Shocked B Haughton, Devon Island	Eocene	4

Table 1 Table of sample locations and ages.

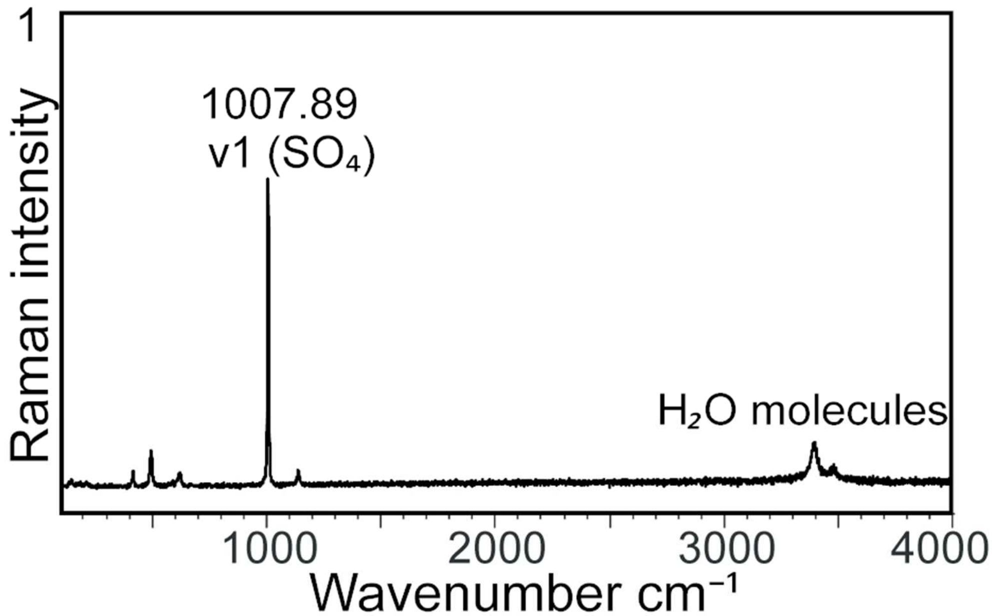

Fig. 1 Extended spectra 100-4000 cm^{-1} showing v1 sulphate symmetric stretching mode (1007.89 cm^{-1}) and stretching mode of H2O (~3450 cm^{-1}).

80x50mm (300 x 300 DPI)

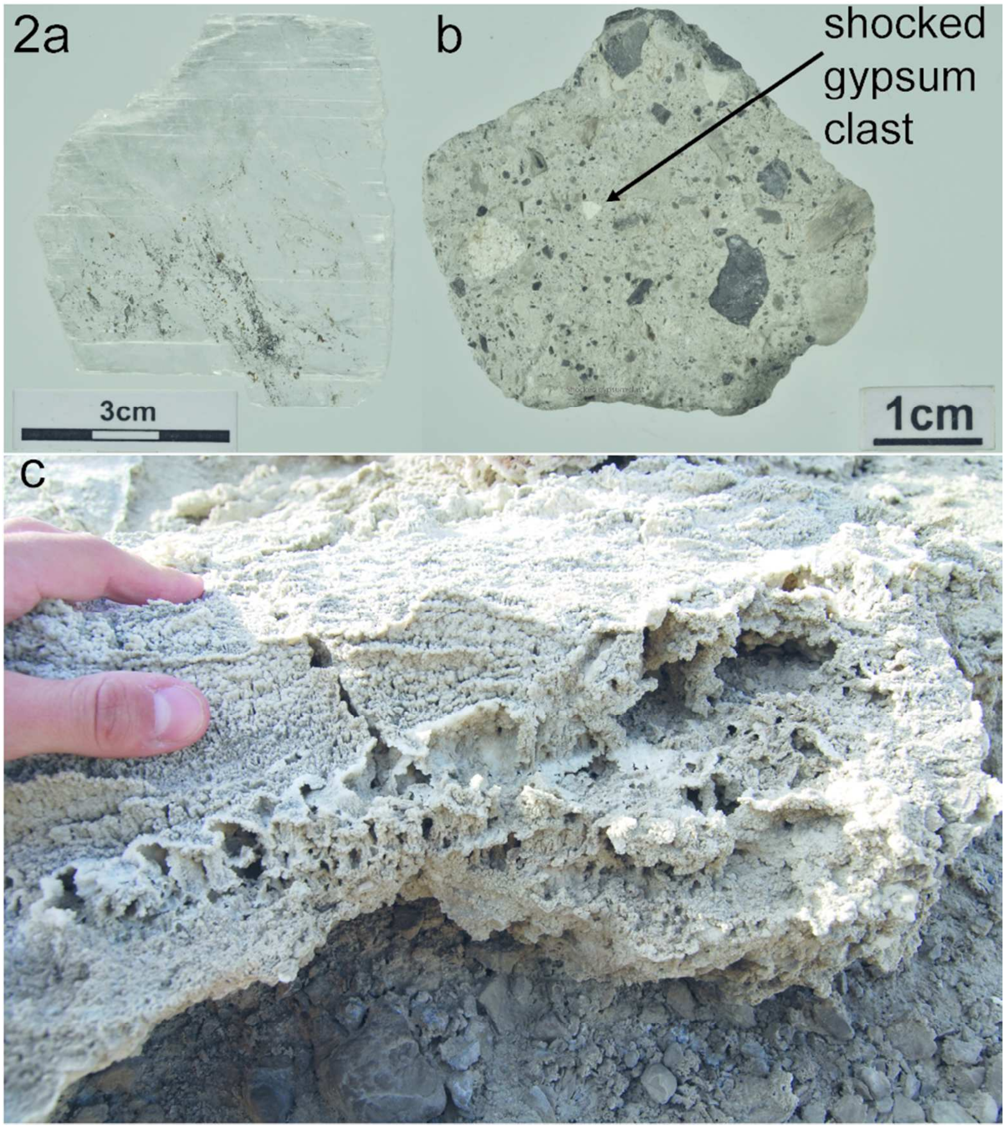

Fig 2. Sample photographs. (a) Selenite, Haughton crater (S2), showing black pigmentation of bacterial colonies. (b) Melt breccia, Haughton crater (SH1), showing fragment of shocked gypsum. (c) Evaporitic gypsum crust, Haughton crater (C1).

80x90mm (300 x 300 DPI)

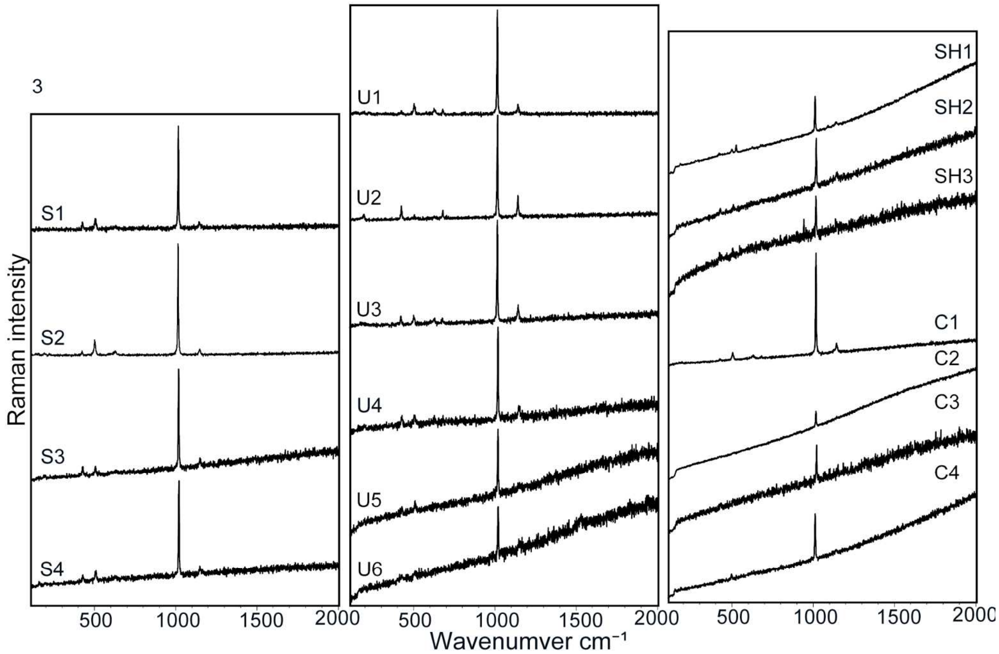

Fig 3. Extended Raman spectra for gypsum (100-2000 cm^{-1}). X axis is Raman shift in reciprocal centimetres (cm-1). Y axis is Raman intensity in arbitrary units (a.u.). 'SH' spectra have experienced shock from meteoric impact. 'C' spectra are gypsum samples which have been dissolved then re-precipitated as evaporitic crusts. 'S' spectra are selenite, a transparent form of gypsum. 'U' spectra are from unaltered gypsum samples unaffected by shock or dissolution and re-precipitation.

175x116mm (300 x 300 DPI)

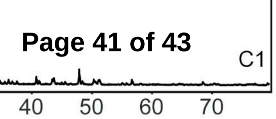
C1
40
50
60
70

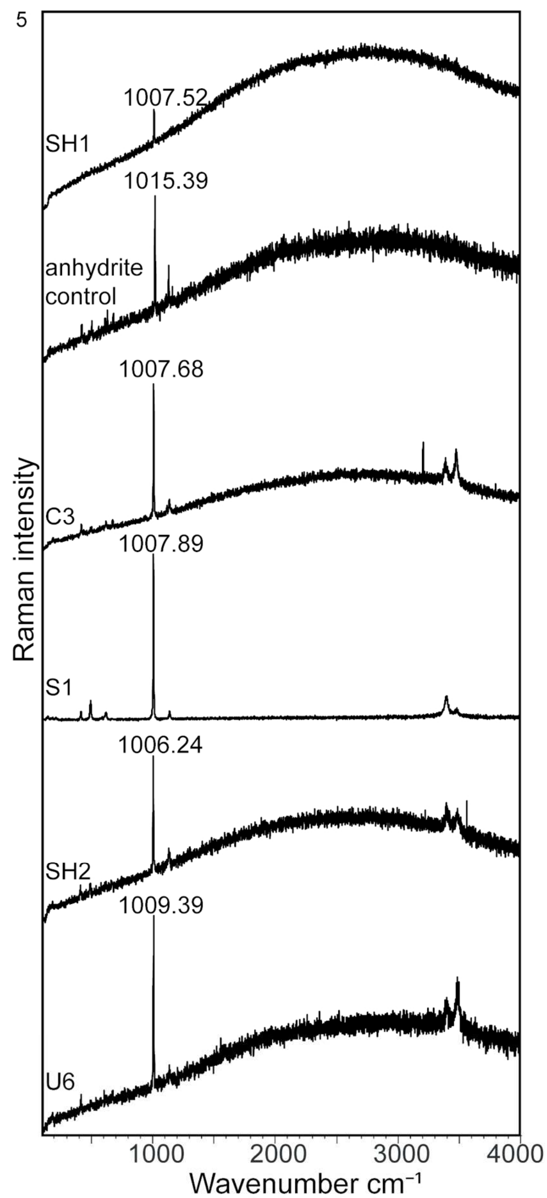

Fig 5. Extended Raman spectra for gypsum and anhydrite (100-4000 cm^{-1}). Spectra include v1 sulphate stretching mode and H2O molecule stretching mode around 3500 cm^{-1}.

80x176mm (300 x 300 DPI)

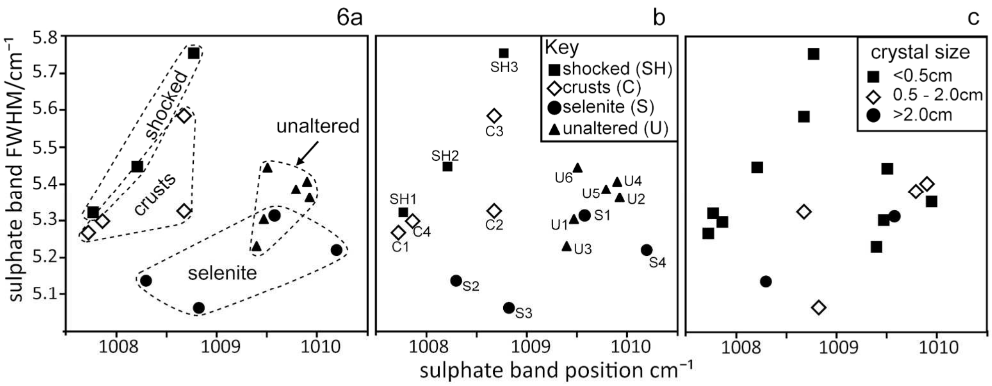

Fig 6. Sulphate band position against sulphate band FWHM. x-axis, is the sulphate (v1) band position in reciprocal centimetres (cm^{-1}). Y-axis, is the sulphate (v1) full width at half maximum (FWHM). (a) Samples are separated into their geological groups. (b) Samples are distinguished by sample classification (table 1). (c) Samples are distinguished based on crystal size. Squares denote a crystal size less than 0.5 cm; diamonds denote a crystal size of between 0.5 and 2 cm; circles denote a crystal size greater than 2 cm.

175x67mm (300 x 300 DPI)